

Time-Series InSAR Applications Over Urban Areas in China

Daniele Perissin and Teng Wang

Abstract—In this study, we present the results achieved within the Dragon project, a cooperation program between the European Space Agency (ESA) and the National Remote Sensing Center of China (NRSCC), about monitoring subsidences and landslides in urban areas, analyzing cities growth and measuring the deformation of big man-made structures. Among the processed areas, we report here the main results we obtained in the test sites of Shanghai, Tianjin, Badong, and Three Gorges Dam. The techniques that have been used to process the data are original SAR interferometry (InSAR), Permanent Scatterers (PS-InSAR), Quasi-PS InSAR (QPS-InSAR), and a combination of coherent-uncoherent analysis. The results show that time-series InSAR techniques allow us to extract ground information with high spatial density and thus help us understanding the impact of urban development on terrain movements.

Index Terms—Synthetic aperture radar interferometry (InSAR), Three Gorges Project (TGP), time-series analysis, urban development.

I. INTRODUCTION

AS THE largest developing country in the world, China has been in an era of rapid urbanization since the 1980s. Generally speaking, urban areas in China are developing in two main ways: urban expansion and new city construction. For the first mode, many metropolises are developing rapidly in both population and extension. The increasing amount of skyscrapers press the alluvial plains along the river deltas in east China. Moreover, water resources are needed more and more, and underground water is overpumped in many developed areas. As a consequence, in China, many cities have been suffering different kinds of land subsidence since the end of the last century [1].

At the same time, together with huge infrastructures, many new cities are being built. The Three Gorges Project (TGP) is without any doubt the most significant example in China: a dam has been built on the Yangtze river, increasing the water level over 100 m, flooding huge areas and changing the face of the entire region facing the river. The dam and its surroundings formed

Manuscript received October 31, 2009; revised March 16, 2010. This work was supported in part by the National Key Basic Research and Development Program of China under Contract 2007CB714405 and Contract 2006CB701304 and the Nature Science Foundation of China under Contract 40721001.

D. Perissin is with the Institute of Space and Earth Information Science, Chinese University of Hong Kong, Hong Kong, China (e-mail: daniele.perissin@cuhk.edu.hk).

T. Wang is with the State Key Laboratory for Information Engineering in Surveying, Mapping and Remote Sensing, Wuhan University, Wuhan 430079, China, and also with the Dipartimento di Elettronica e Informazione, Politecnico di Milano, 20133 Milan, Italy (e-mail: wang.teng@gmail.com).

Color versions of one or more of the figures in this paper are available online at <http://ieeexplore.ieee.org>.

Digital Object Identifier 10.1109/JSTARS.2010.2046883

an urban-like area themselves. Besides many artificial structures such as the dam body, navigation instruments, and power plants, many thousands of staff members and tourists are hosted within the dam site. Immigrants moved en masse toward the area, and many cities have been rebuilt at higher locations. The high pressure of the reservoir on the riverbed and the water infiltration affection cause potential crust instability. Dam stability and landslides over the cities along the Yangtze have to be monitored regularly.

Usually, remote sensing of urban areas focuses on change detection and land use mapping [2], and results represent the rapid urban expansions, especially in developing countries like China [3]–[5]. However, impacts of urban development such as subsidence, are rarely studied in this field. Synthetic aperture radar interferometry (InSAR) allows us measuring the terrain movement with radar observations acquired by satellites [6], [7]. Main drawbacks of InSAR are geometric and temporal decorrelation [8], [9] as well as atmospheric disturbances that affect the radar signal [10].

Aiming at solving the restrictions of InSAR, the Permanent Scatterers technique (PS-InSAR) [11], [12] was invented and developed at the Politecnico di Milano (POLIMI) in the late 1990s. Instead of extracting information from the whole SAR image, PS-InSAR exploits long temporal series of acquisitions to identify point-like stable reflectors (PSs). The electromagnetic stability of PSs allows obtaining around 1-m accuracy DEMs [13] and millimetric estimates of terrain motion [14]. Recently, by considering different interferometric combinations, the Quasi-PS (QPS) technique was presented [18] to extract information also from distributed and decorrelating targets.

Since a good knowledge of the PS physical nature is a key step for the correct interpretation of the measured deformation mechanism, the physical nature of the targets has been investigated in [19]–[21]. The association of each coherent pixel to an actual target is achieved by exploiting all the measures with time series of InSAR images. Since PSs are the stable artificial targets, which can be usually found in urban areas, their lifetime and density can be used to describe the urban development with spatial and temporal context. With a regular revisiting cycle, the benefits that can be gained from time series of InSAR images are in two aspects: 1) since the PS is related to artificial targets, different PS birth time that represents the urban growth can be obtained with the ground displacement and 2) each PS can be related to the physical characteristics of the single target.

The work presented here has been carried out within the Dragon I and II cooperation projects between the European Space Agency and the National Remote Sensing Center of China (ESA and NRSCC, respectively). In this framework, the “topographic measurement” group has been working on PS

analysis in several urban test sites in China, getting ground deformation maps of wide areas, till differential movements over single constructions. The time-series InSAR images used in this paper were acquired by the ESA satellites, namely European Remote Sensing 1/2 (ERS-1/2) and Envisat. For the images from both satellites, the ground resolution is around 5 m in azimuth and 25 m in range; the bandwidths are around 16 MHz. The main difference between ERS and Envisat ERS-like acquisitions is the carrier frequency (5.3 GHz for ERS-1/2 and 5.331 GHz for Envisat). Thanks to the increasing amount of the archived ESA SAR images, which allow us to measure the rapid development of China since the 1990s, examples of urban deformation monitoring are reported here.

II. TIME-SERIES IN SAR ANALYSIS METHODS

Here, we give a very brief review of the core ideas of PS and QPS techniques, neglecting algorithm details. The interested readers may refer to [11], [12], and [18] for more information.

The PS-InSAR technique first searches for pixels with high amplitude stability, called PS candidates (PSCs), from a long time series of InSAR images. For each PSC, the different phase contributions (dependent on elevation, motion, and atmospheric noise) are separated, exploiting their different spatial and temporal characteristics. Atmospheric phase artefacts are then interpolated for each image to produce the water vapor concentration at the SAR acquisition time [11]. The final PSs are identified by evaluating the dispersion of phase residuals through the temporal coherence [12]. The precision of the measures depends on the coherence and on the deviation of normal and temporal baselines.

In the PS analysis [11], the interferometric phase is generated by referring all images to a common Master acquisition. In order to extract information also from partially coherent targets, various techniques have been developed, including those presented in [15]–[18]. From its side, the QPS technique finds the best set of image pairs by maximizing the interferometric coherence [22] of the graph connecting all images at hand. Since the subset of coherent interferograms that carry information can be different from point to point within the analyzed scene, a subset of coherent interferograms for each point has to be considered. To this purpose, the absolute value of the spatial coherence is chosen as a weight in the estimation process, thus only coherent interferograms for a given point cooperate to determine the result. Moreover, the phase of the spatial coherence is used instead of the unfiltered pixel phase to enhance the signal-to-noise ratio. Finally, like in the PS technique, topography and displacement can be jointly estimated from the subset of filtered coherent interferograms. The QPS technique can be implemented by operating some relatively small changes in the classical PS processing chain [11], with considerable advantages in partially coherent areas.

The QPS technique can be considered to be complementary with the PS technique, and one will be preferred to the other according to constraints and requests of the case study at hand. In Section III, we show the results of the PS processing in the cities of Shanghai and Tianjin. In Section IV, the slow landslide monitoring results in Badong and the deformation measures over the

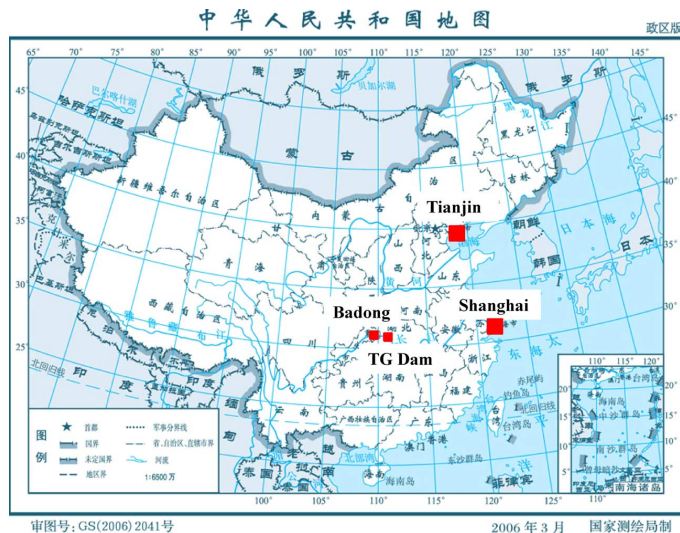


Fig. 1. Locations of Shanghai and Tianjin, Badong, and Three Gorges Dam in China. The map of China comes from the Chinese State Bureau of Surveying and Mapping.

Three Gorges Dam are obtained with the QPS technique. In this paper, we present the results together highlighting the potentiality for urban applications of the applied methodologies.

III. METROPOLIS DEVELOPMENT AND SUBSIDENCE MONITORING

In China, the rate of population living in urban areas increased from 18% to 45% in the last three decades [23]. The rapid development of Chinese urban areas causes environmental problems and even geologic hazards [1]. In the following two sections, we present the time-series InSAR analysis results over two metropolises and two newly formed cities. The locations of these four test sites are shown in Fig. 1. All of these selected areas are very typical of both the urbanization and expansion of the 1990s. Also, the selection of the test sites depends on the availability of the archived data from ESA satellites.

A. Shanghai

Shanghai is the largest city in China and one of the largest metropolitan areas in the world, with over 20 million people. At the beginning of the Dragon Project in 2004, Shanghai was selected as the first PS analysis test site in China for studying the subsidence caused by underground water pumping and by the rapid city development in the 1990s. Thanks to the archived ERS data of ESA, 40 images spanning the interval 1993–2000 were processed. The results of the PS analysis allow detecting areas around the urban center of Shanghai. In this area, some targets was subsiding with a linear trend of even more than 40 mm per year. The PS measures were then compared with the deformation map retrieved by means of leveling data in Shanghai, revealing quite good agreement.

Fig. 2 shows the most significant outcomes of the analysis. In Fig. 2(a), the geocoded linear deformation trend in Shanghai is reported. Each point represents a permanent scatterer and the color scale (online version) indicates the average linear motion,

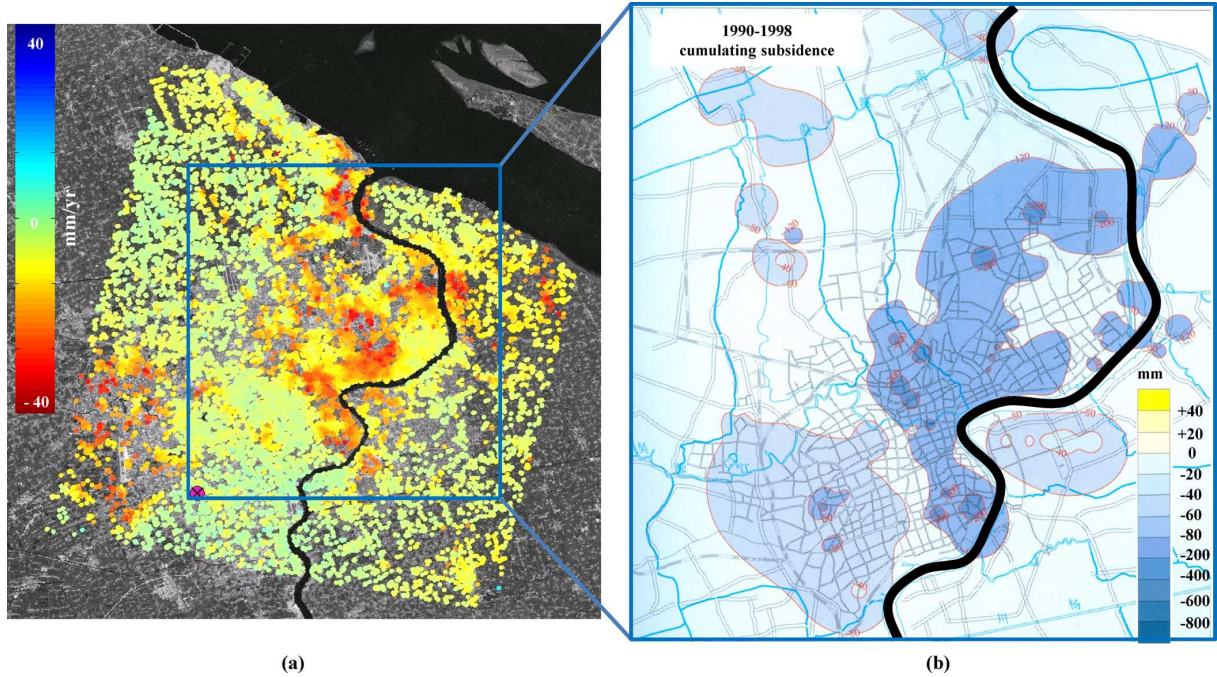


Fig. 2. Comparison between deformation rate measured by (a) the PS technique and (b) optical leveling, where the cumulating subsidence map is interpolated from the leveling measured points in the urban area of Shanghai [24].

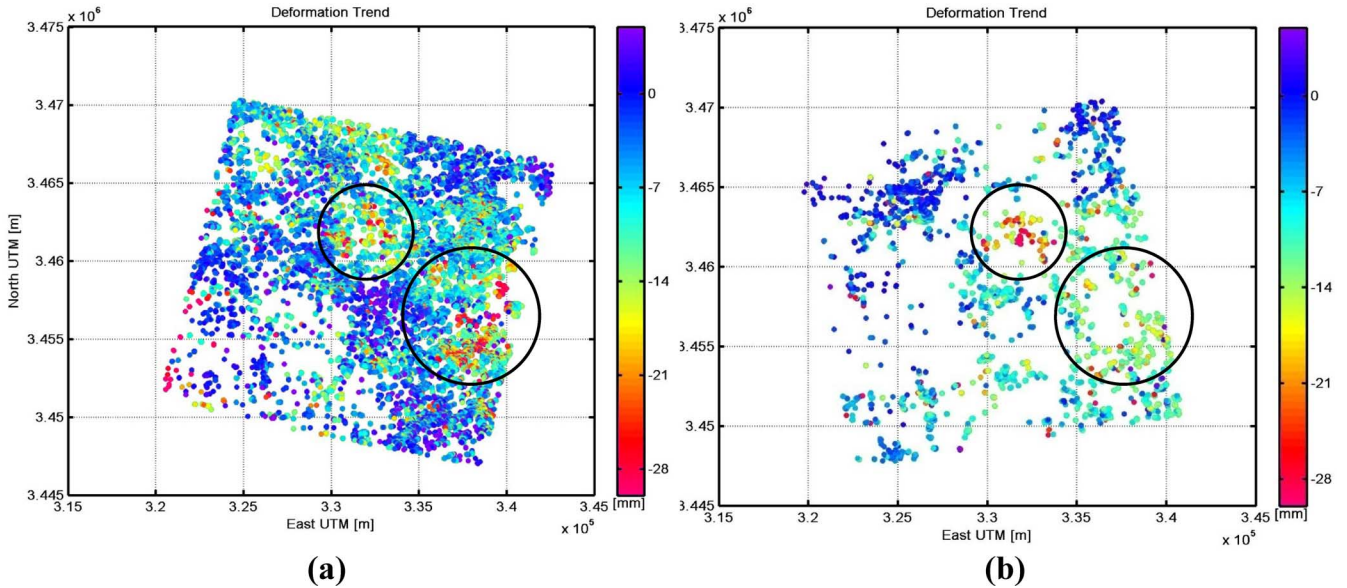


Fig. 3. Comparison between PS velocity field estimated with (a) ERS data and (b) Envisat data acquired from the parallel tracks 268 and 497. Black circles identify the two areas with the highest subsidence rate.

spanning between -40 – 40 mm/year. In Fig. 2(b), the deformation rate interpolated from the optical leveling techniques is shown [24]. The Yangtze River is indicated with the black curve for better understanding the comparison. The two maps are pretty in accordance, highlighting the strongest motions near a branch of the mouth of the Yangtze River, with a maximum subsidence rate of -40 mm/year. The displacement time series of ten leveling benchmarks have been compared with those of the PS closest to them. The standard deviation between the two measures is less than 2 mm/year [25].

The positive results obtained in Shanghai drew the interest to monitoring its urban ground stability also after the year 2000. Considering the loss of gyroscopes of ERS-2 and the difficulty in connecting ERS and Envisat data together (not only for the different carrier frequencies, but mostly because of the city development), the problem of carrying out a PS analysis with few Envisat images per track was tackled. The studies on the physical nature of PSs in urban sites suggested then as solution the exploitation of multi-angle targets as dihedrals to combine data acquired from parallel tracks [25]. In this way, it was possible to double the number of data samples to estimate height and de-

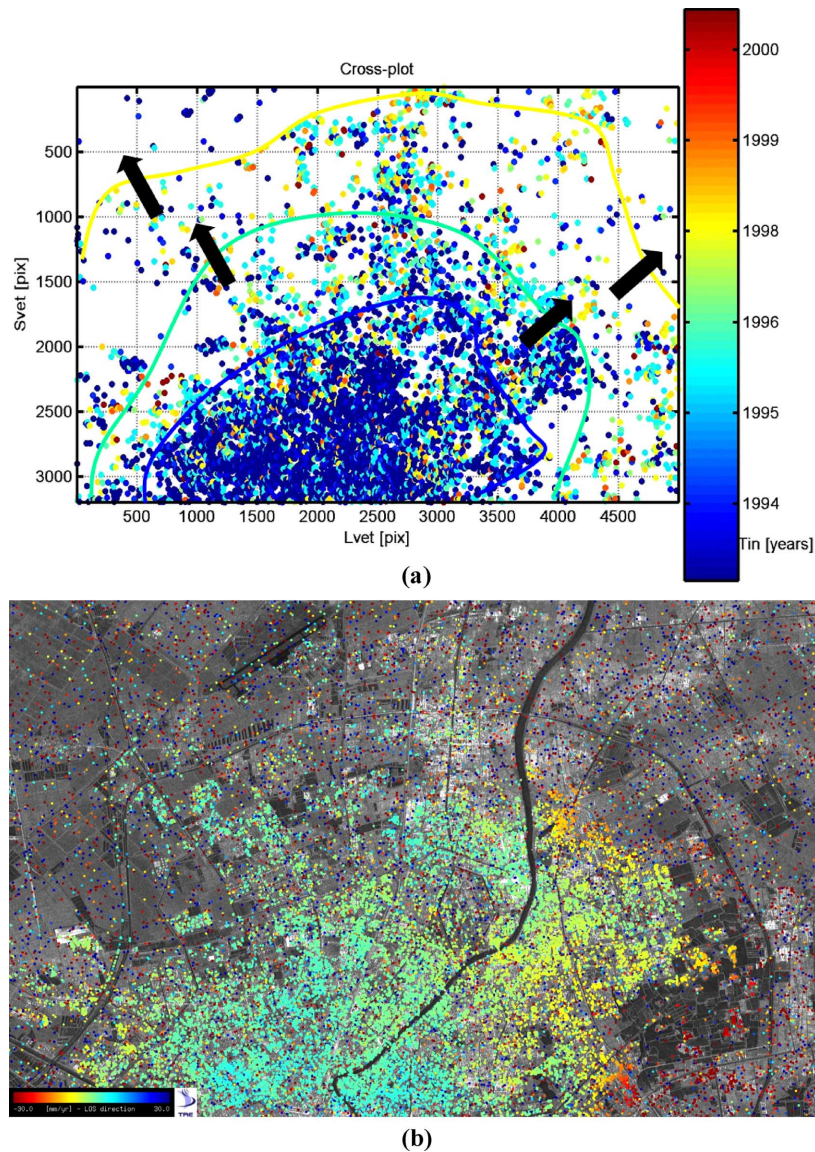


Fig. 4. About 10 000 PSs detected in the Tianjin test site. (a) The birth date of PS (shown with different colors in the online version), indicating the development of the urban area. The colored (online version) contour lines corresponds to the average PS birth date. (b) The measured deformation trends. Color scale (online version): average deformation trend (−30–30 mm/year).

formation trends of dihedrals. The developed method allowed updating the subsidence monitoring in Shanghai. The results, which identify the same sinking areas of the ERS analysis, reveal a general decrease of deformation rate.

Fig. 3 brings the main achievements of the study over a limited processed area. In Fig. 3(a), the deformation map estimated with ERS data along a descending track (n. 3) is shown in geographical coordinates. In Fig. 3(b), the same area has been processed using Envisat data taken from two ascending parallel tracks (n. 268 and 497), with 14 and 12 available images, respectively. As is visible from Fig. 3, the number of detected targets is strongly reduced than in a classical analysis, since only dihedron-like scatterers are coherently imaged. Nonetheless, a reasonable agreement is found between the subsiding areas in the two datasets (the two reported circles). Moreover, in the right circle, it can be noted that the average rate is lower in the map retrieved with parallel tracks than in the other one.

B. Tianjin

Along with the successful application of the PS-InSAR technique in Shanghai, Tianjin was selected as other testbed. As the third directly controlled municipality in China, Tianjin developed rapidly in the 1990s and suffered subsidence problems due to underground water overextraction and coal mining. In this test site, besides estimating the PS height and deformation trends, an investigation on the urban targets physical nature has been carried out by exploiting 23 ERS images. By analyzing the amplitude history of SAR images, birth and death days of PSs were also extracted to recognize the growth pattern of the city. The subsiding area was detected being confined to the surroundings of the city center [26]. This is a change detection technique that analyzes amplitude time series rather than couple of images. Moreover, taking into account the targets scattering pattern, eventual intensity fluctuations due to the acquisition ge-

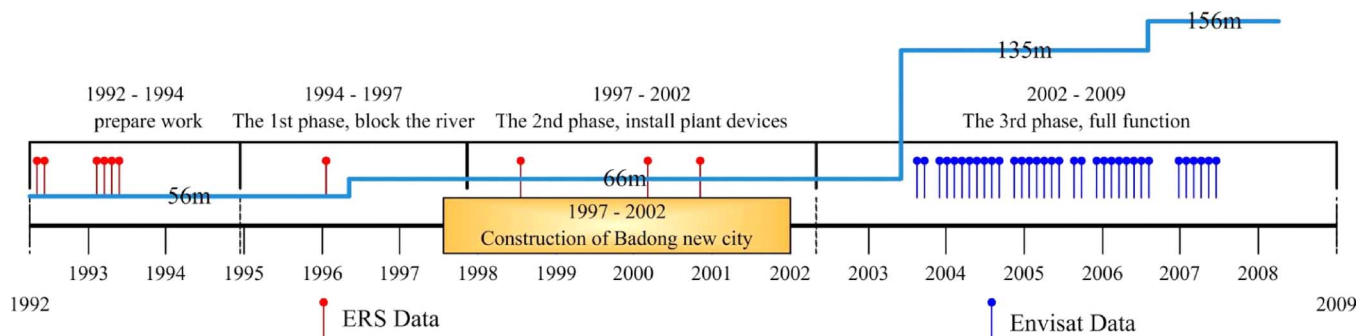


Fig. 5. History of the different phases of the TGP. Blue line (online version): water level of the Yangtze river. Red (blue) stems (online version): ERS (Envisat) data acquired over the dam.

ometry are compensated for. The consequence is a much higher reliability and robustness of the estimate.

From Fig. 4(a), it is possible to notice the still rural character of the suburban area of Tianjin at the time of the acquisitions by looking at the density of PS. The arrows indicate the main developing directions of Tianjin in the 1990s. By calculating the average birth date on a regular grid, we can find a general trend increasing with the distance from the city center. The contour lines with different average birth date describe the trend we obtained from time-series InSAR analysis. On the other hand, the center of the urban area appears to be mostly stable, while along the river and, in particular, in the lower right corner of the image the highest concentration of sinking targets lies as shown in Fig. 4(b). The analysis in Tianjin was performed with a very low number of images and even more with a sparse temporal sampling. Notwithstanding, the outcome of the work is particularly meaningful and highlights the motions affecting the imaged terrain.

IV. SLOW LANDSLIDES AND DAM STABILITY MONITORING OVER THE THREE GORGES REGION

Three Gorges is an overall name given for a series of gorges from Fengjie, Chongqing municipality, to Yichang, Hubei province, along the Yangtze river in China. From west to east, the three most famous gorges are QuTang Gorge, Wu Gorge, and XiLing Gorge. Since Yangtze is a seasonal river, floods happen each raining season (from May to October); in the downriver plains, for example, Jiangnan plain is endangered almost every five years. Actually, the most important objective for constructing TGP is to control the seasonal floods of the Yangtze by releasing or storing the water. In the meantime, clean electricity power can be generalized by the different water levels up- and down-river of the dam.

In Fig. 5, the history of the phases of the TGP is diagrammed together with the height level of the Yangtze river. Red and blue stems (online version) are plotted in correspondence of the acquisition dates of ERS and Envisat images, respectively. The 40 Envisat images used in the following discussions fall in the third phase of the project. It is worth noticing that, in the middle of 2006, the construction of all of the power plants were finished and the water level was increased around 20 m to generalize more hydropower.

A. Badong

Badong is settled on the river side of the Yangtze River, in Hubei province. It is located just between the Wu and Xiling Gorges. The old town of Badong has a history of more than 1500 years. Unfortunately, due to the construction of TGP, this town was going to be under the rising water and the emigration of the whole town was organized in the summer of 1997. Almost all buildings of the old town were demolished. Meanwhile, a new town that covers about 7.3 km² with more than 50 000 residences began to form in 2002. Since ERS and Envisat data were acquired before and after the construction of the dam, the changes of the river in this area can be observed from the reflectivity maps of the data sets of two sensors. Fig. 6 shows the incoherent average reflectivity maps of (a) ERS and (b) Envisat data. The Yangtze river can be seen as much wider in the Envisat image, and the urban changes due to the population migration are identified by the red rectangle.

Since the town was built along the steep river banks, landslide monitoring is a very important task for the whole area. Actually, many consolidation works were settled for landslide protection in Badong. As shown in Fig. 7, two subsidence regions in the south river bank of Badong city are identified by the QPS technique. One is in the west part of the city, about 400 m above the Yangtze river. Another region is in the east part of the city near the river. With the achieved QPS density of measures, the borders of residential areas are easy to be identified. Moreover, the area in the south east of the city is also found being affected by terrain instability.

B. Dam Site

The Three Gorges Dam is located near San Dou Ping town in the east exit of the Three Gorges region. The main structure of the TGP consists of three parts: the dam, hydrological generator plants and navigation instruments. The body of the dam is 2355 m long and 185 m high. The bottom and top of the dam are respectively 115 and 40 m wide. The spillway is in the middle of the dam where the main river canal was. The sluice gates installed on the bottom of the dam are used to control the capability of the upstream reservoir and wash the alluvial sands to the downstream area. The power plant houses, flanking the spillway (left and right riverbank), accommodate altogether 26 sets of turbine generators.

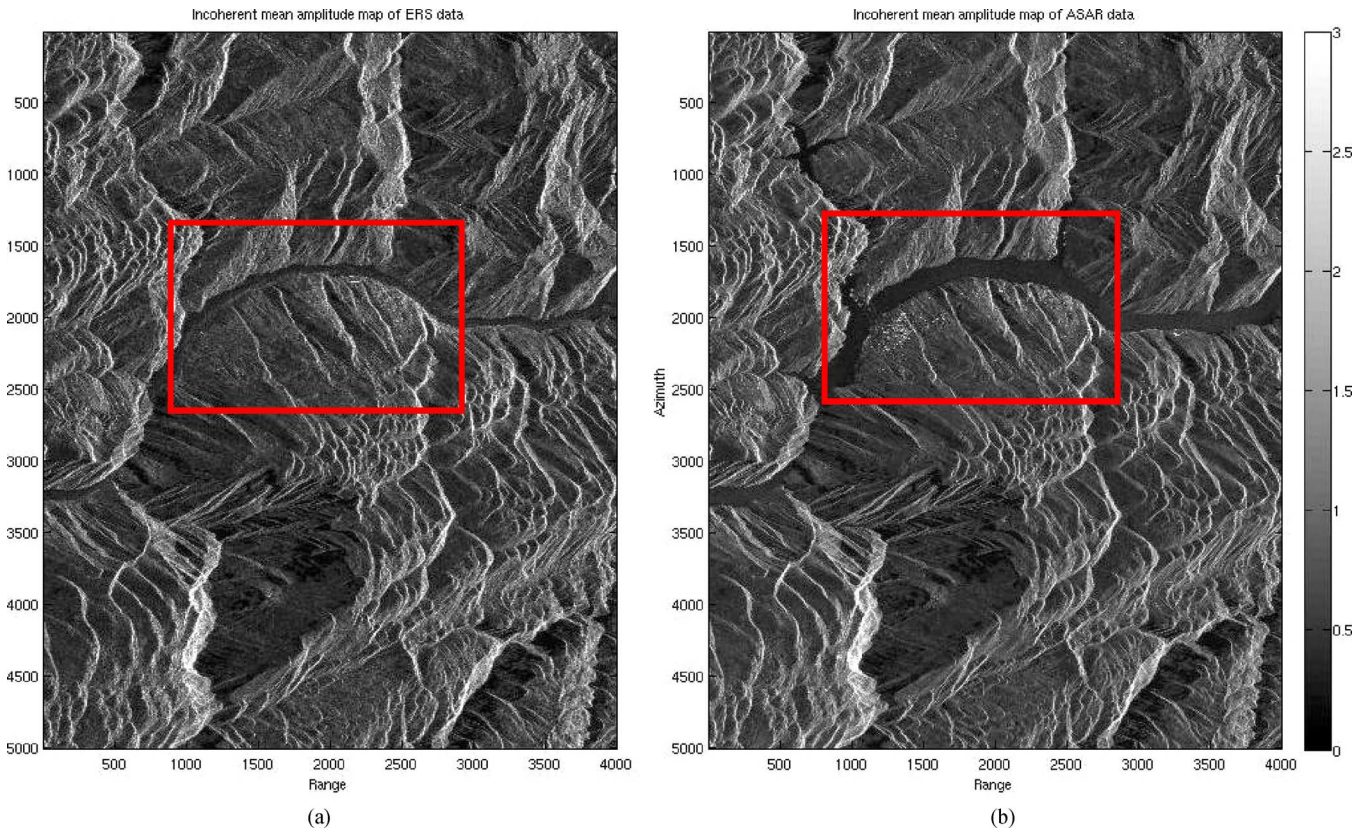


Fig. 6. Reflectivity maps of Track 75 Frame 2979 from (a) ERS images and (b) Envisat images. The red rectangle (online version) indicates the new city of Badong, which is brighter in the Envisat image because of the urbanization. The Yangtze river is much wider in the Envisat image because of the TGP.

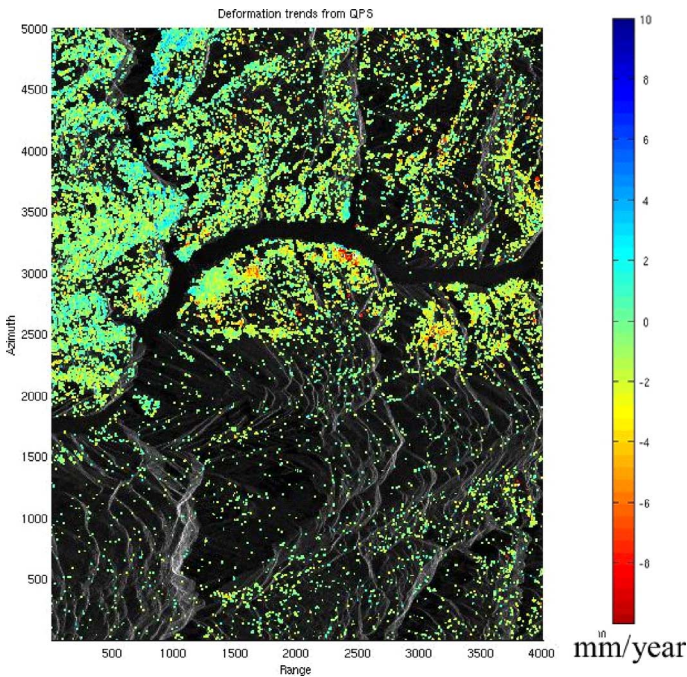


Fig. 7. Deformation trends obtained from QPS analysis. Two slow landslides areas are identified.

By looking at the reflectivity map of the analyzed area in Fig. 8, the structure of the dam crossing the river can be easily recognized. Four matrices are visible, reporting the amplitude

behavior of four scatterers in the whole SAR dataset. Each pixel of a matrix identifies a pair of images. Blue (online version) indicates that the amplitude of the scatterer is similar in the two images, and yellow and red (online version) mean that a change happened. Thus, from the amplitude matrix of the ship lift, it is possible to recognize the two states of the lift, up and down, that change the backscattered signal. The left power plant in the reflectivity map is the north plant and was built before 2002. The amplitude matrix in Fig. 8 of a scatterer in the north side shows a constant pattern in the processed time span. The right part of the dam was under construction, the third matrix shows the birthday of the target in the construction site, and the fourth matrix shows a target on the cofferdam, which was dismantled in 2006.

The elevation and deformation trends over the dam site are estimated with the QPS technique and shown in Fig. 9(a) and (b). Since we cannot find any published topographic map in this area, the validation of the results are carried out by comparing the results on some known locations: 1) the tail water platform of the left part of the dam is 83.5 m; 2) the top of the left plant house is 117.2 m; 3) the top of the dam is 185 m; and 4) the spillway weir is 158 m. As shown in Fig. 9(a), the estimated elevation from QPS technique fit close to the ground truth. In addition, since the downriver part of the dam faces the satellite LOS, the elevation of the left dam can be represented as three parts: the tail water platform, the top of the plant house, and the top of the dam. The lifting equipment on the top of the dam show about 200 m elevation. Near the permanent ship locks, although

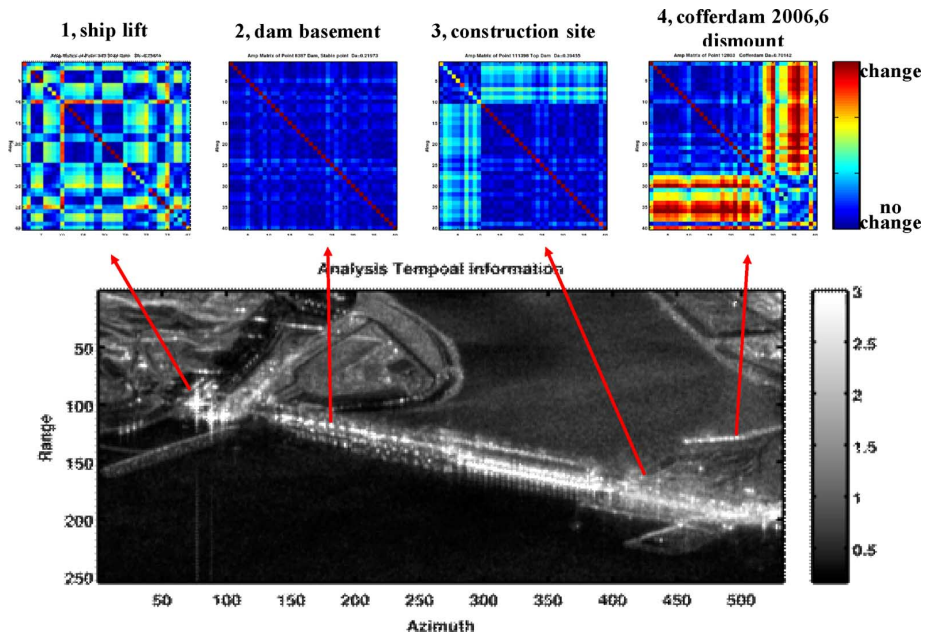


Fig. 8. Reflectivity map of the Three Gorges dam and different scatterer's signatures derived from the amplitude of SAR images. In each matrix, a pixel identifies a couple of images. Blue (online version) means no change of amplitude among the couple and yellow and red (online version) mean progressively increasing changes. The amplitude series for each pixel was shown as the matrix diagonal.

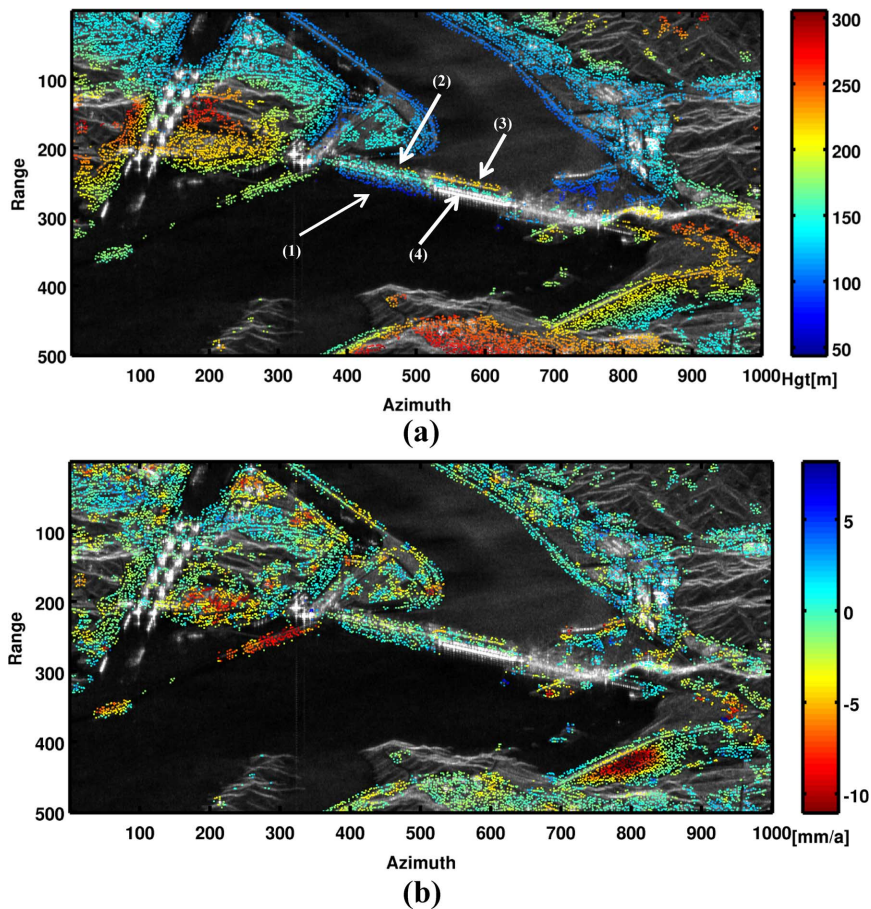


Fig. 9. (a) The measured elevation and (b) deformation trends over the dam site. The numbers on (a) indicate: 1) the tail water platform of the left part of the dam; 2) the top of the left plant house; 3) the top of the dam; and 4) the top of the spillway.

not that many QPS points are present, the five levels of the ship locks can be observed.

From the results shown in Fig. 9(b), over the dam, only slight deformation trends can be observed. In other words, the Three

Gorges dam is quite stable during the time span of our data set. From the obtained deformation trends, on the top of the left part of the dam, the slight deformation trends are apart from the satellite, on the contrary, the power plant on the bottom of the dam shows the deformation trends towards the satellite. We presume that the dam declined slightly on account of the upriver water pressure over the riverbed crust.

In the dam surroundings, we detected several subsidence areas in the left riverbank, especially along the axis of the dam to the area between the ship lift and permanent ship locks. We presume that the construction of the navigation establishments changed the distribution of the underground water and caused superficial subsidence. In addition, several slight subsidence areas can be observed near the Yangtze River. Synthetically, superficial subsidence often happens near the water area of Yangtze, the maximum subsidence appears on the upriver embankment near Zigui county. The highest subsidence velocity is over 10 mm/year.

V. CONCLUSION

In this paper, we have shown some results obtained within the cooperation Dragon program for what concerns urban terrain motion monitoring. PS and QPS techniques allow measuring the average deformation trend of man-made structures, revealing subsidences or the stability of single buildings. The validation work have been carried out in two aspects: 1) the Shanghai subsidence monitoring results are cross-validated with the optical leveling measures and 2) the elevation measured by the QPS technique is validated with the well-known points on the Dam. The present results show the potentiality of time-series analysis of InSAR images for urban area monitoring in China, and for example, the time-series InSAR images and techniques have been successfully applied in the Shanghai Institute for Geology Survey for monitoring the subsidence over this city annually. As future work, we are also contacting relative local government and institutes for collecting deformation measures from other techniques (e.g., leveling and GPS) to validate and enhance our results. Moreover, the quality and quantity of information that can be extracted with such techniques from C-band data arouses great expectation towards the future availability of time series of X-band images as taken by TerraSAR-X or Cosmo SkyMed.

ACKNOWLEDGMENT

The authors are very thankful to ESA for the Envisat and ERS data provided under the Dragon project and to T.R.E. TeleRilevamento Europa for focusing and registering SAR data. The authors would also like to thank the SAR group of the Electronic and Information Department of the Politecnico di Milano, Milan, Italy, lead by Prof. Rocca and Prof. Prati.

REFERENCES

- [1] D. Ge, Y. Wang, L. Zhang, Y. Wang, and Q. Hu, "Monitoring urban subsidence with coherent point target SAR interferometry," in *Proc. 2009 Joint Urban Remote Sensing Event*, 2009, pp. 1–4.
- [2] P. Gamba, F. Tupin, and Q. Weng, "Introduction to the issue on remote sensing of human settlements: Status and challenges," *IEEE J. Sel. Topics Appl. Remote Sens.*, vol. 1, no. 2, pp. 82–86, Jun. 2008.
- [3] X. Tong, S. Liu, and Q. Weng, "Geometric processing of QuickBird stereo imageries for urban land use mapping: A case study in Shanghai, China," *IEEE J. Sel. Topics Appl. Remote Sens.*, vol. 2, no. 2, pp. 61–66, Jun. 2009.
- [4] L. Jiang, M. S. Liao, H. Lin, and L. Yang, "Synergistic use of optical and InSAR data for urban impervious surface mapping: A case study in Hong Kong," *Int. J. Remote Sens.*, vol. 30, no. 11, pp. 2781–2796, 2009.
- [5] T. Wang, M. Liao, and D. Perrissin, "Coherence decomposition analysis," *IEEE Geosci. Remote Sens. Lett.*, vol. 7, no. 1, pp. 156–160, 2010.
- [6] A. K. Gabriel, R. M. Goldstein, and H. A. Zebker, "Mapping small elevation changes over large areas: differential radar interferometry," *J. Geophys. Res.*, vol. 94, pp. 9183–9191, 1989.
- [7] R. F. Hanssen, *Radar Interferometry. Data Interpretation and Error Analysis*. Dordrecht, The Netherlands: Kluwer, 2001.
- [8] H. A. Zebker and J. Villasenor, "Decorrelation in interferometric radar echoes," *IEEE Trans. Geosci. Remote Sens.*, vol. 30, no. 5, pp. 950–959, Sep. 1992.
- [9] F. Gatelli *et al.*, "The wavenumber shift in SAR interferometry," *IEEE Trans. Geosci. Remote Sens.*, vol. 32, no. 4, pp. 855–865, May 1994.
- [10] H. A. Zebker, P. A. Rosen, and S. Hensley, "Atmospheric effects in interferometric synthetic aperture radar surface deformation and topographic maps," *J. Geophys. Res.*, vol. 102, pp. 7547–7563, 1997.
- [11] A. Ferretti, C. Prati, and F. Rocca, "Permanent scatterers in SAR interferometry," *IEEE Trans. Geosci. Remote Sens.*, vol. 39, no. 1, pp. 8–20, Jan. 2001.
- [12] C. Colesanti, A. Ferretti, F. Novali, C. Prati, and F. Rocca, "SAR monitoring of progressive and seasonal ground deformation using the permanent scatterers technique," *IEEE Trans. Geosci. Remote Sens.*, vol. 41, no. 7, pp. 1685–1701, Jul. 2003.
- [13] D. Perissin, "Validation of the sub-metric accuracy of vertical positioning of PS's in C band," *IEEE Geosci. Remote Sens. Lett.*, vol. 5, pp. 502–506, 2008.
- [14] A. Ferretti, G. Savio, R. Barzaghi, A. Borghi, S. Musazzi, F. Novali, C. Prati, and F. Rocca, "Submillimeter accuracy of InSAR time series: Experimental validation," *IEEE Trans. Geosci. Remote Sens.*, vol. 45, no. 5, pp. 1142–1153, May 2007.
- [15] P. Bernardino, G. Fornaro, R. Lanari, and E. Sansosti, "A new algorithm for surface deformation monitoring based on small baseline differential SAR interferograms," *IEEE Trans. Geosci. Remote Sens.*, vol. 40, no. 11, pp. 2375–2383, Nov. 2002.
- [16] A. Hooper, H. Zebker, P. Segall, and B. Kampes, "A new method for measuring deformation on volcanoes and other natural terrains using InSAR persistent scatterers," *Geophys. Res. Lett.*, vol. 31, no. 23, pp. 1–5, 2004.
- [17] F. De Zan and F. Rocca, "Coherent processing of long series of SAR images," in *Proc. IEEE Int. Geosci. Remote Sens. Symp.*, Jul. 25–29, 2005, vol. 3, pp. 1987–1990.
- [18] D. Perissin, A. Ferretti, R. Piantanida, D. Piccagli, C. Prati, F. Rocca, A. Rucci, and F. de Zan, "Repeat-pass SAR interferometry with partially coherent targets," in *Proc. Fringe*, Frascati, Italy, 2007, pp. 1–7.
- [19] D. Perissin, C. Prati, M. E. Engdahl, and Y. L. Desnos, "Validating the SAR wavenumber shift principle with the ERS Envisat PS coherent combination," *IEEE Trans. Geosci. Remote Sens.*, vol. 44, no. 9, pp. 2343–2351, Sep. 2006.
- [20] D. Perissin and A. Ferretti, "Urban target recognition by means of repeated spaceborne SAR images," *IEEE Trans. Geosci. Remote Sens.*, vol. 45, no. 12, pp. 4043–4058, Dec. 2007.
- [21] D. Perissin and F. Rocca, "High accuracy urban DEM using permanent scatterers," *IEEE Trans. Geosci. Remote Sens.*, vol. 44, no. 11, pp. 3338–3347, Nov. 2006.
- [22] R. Touzi, A. Lopes, J. Bruniquel, and P. W. Vachon, "Coherence estimation for SAR imagery," *IEEE Trans. Geosci. Remote Sens.*, vol. 37, no. 1, pp. 135–149, Jan. 1999.
- [23] J. Pan, F. Niu, and H. Wei, *Annual Report on Urban Development of China No.2* Social Sciences Academic Press, Beijing, 2009.
- [24] A. Zhang, D. Luo, X. Shen, L. Lv, H. Chen, Z. Wei, X. Yan, and Z. Fang, Y. Shi, *Shanghai Geological Environmental Atlas*. Beijing, China: Geological, 2002.

- [25] D. Perissin, C. Prati, F. Rocca, D. Li, and M. Liao, "Multi-track PS analysis in Shanghai," in *Proc. ENVISAT*, Montreux, Switzerland, Apr. 23–27, 2007, pp. 1–6.
- [26] D. Perissin, A. Parizzi, C. Prati, and F. Rocca, "Monitoring Tianjin subsidence with the Permanent Scatterers technique," in *Proc. Dragon Symp.*, Santorini, Greece, Jun.-Jul. 27–1, 2005, pp. 393–398.
- [27] D. Perissin, T. Wang, C. Prati, and F. Rocca, "PSInSAR analysis over the Three Gorges Dam and urban areas in China," in *Proc. Joint Remote Sens. Event*, Shanghai, China, May 20–22, 2009, pp. 1–5.
- [28] T. Wang, D. Perissin, F. Rocca, and M. Liao, "Three Gorges Dam stability monitoring with time series InSAR analysis," *Science in China Series D: Earth Sciences*, accepted for publication.



Daniele Perissin was born in Milan, Italy, in 1977. He received the M.S. degree in telecommunications engineering and the Ph.D. degree in information technology from Politecnico di Milano, Milan, in 2002 and 2006, respectively.

He joined the Signal Processing Research Group, Politecnico di Milano, in 2002 and, since then, he has been working on the Permanent Scatterers technique (PSInSAR) in the framework of radar remote sensing. Since October 2009, he has been a Research Assistant Professor with the Institute of Space and Earth Infor-

mation Science (ISEIS), Chinese University of Hong Kong. He is the author of a patent on the use of urban dihedral reflectors for combining multisensor synthetic aperture radar data, which is his main interest.



Teng Wang received the M.Eng. degree in photogrammetry and remote sensing from Wuhan University, Wuhan, China, in 2006, and is currently working toward the Ph.D. degree in SAR interferometry fields at the State Key Laboratory for Information Engineering in Surveying, Mapping and Remote Sensing, Wuhan University and the Dipartimento di Elettronica e Informazione, Politecnico di Milano, Milan, Italy.

His current research interests include the InSAR and Persistent Scatterer InSAR techniques in moun-

tainous areas.